Physical Science International Journal
4(6): 754-767, 2014

SCIENCEDOMAIN *international*
www.sciencedomain.org

MHD Buoyancy Flows of Cu, Al_2O_3 and TiO_2nanofluid Near Stagnation-point on a Vertical Plate with Heat Generation

Ifsana Karim[1], Md. Sirajul Islam[2] and Md. Shakhaoath Khan[1*]

[1]Department of Chemical Engineering, School of Engineering, University of Newcastle, Callaghan, NSW 2308, Australia.
[2]Department of Mathematics, Bangabandhu Sheikh Mujibur Rahman Science & Technology University, Gopalganj-8100, Bangladesh.

Authors' contributions

This work was carried out in collaboration of all authors. Moreover the funding, computational suggestions, proof reading was also done by all authors and approved the final manuscript.

Original Research Article

Received 17th January 2014
Accepted 7th March 2014
Published 25th March 2014

ABSTRACT

Magnetohydrodynamic mixed convection boundary layer flow of a nanofluid near the stagnation-point on a vertical plate with heat generation is investigated for both assisting and opposing flows are well thought-out. Different types of nanoparticles as copper (Cu), alumina (Al_2O_3) and titania (TiO_2) considering here. Using similarity approach the system of partial differential equations is transformed into ordinary differential equations which strongly depend on the magnetic parameter (M), buoyancy parameter (λ), Prandtl number (P_r), heat generation parameter (Q) and volume fraction parameter (φ). The coupled differential equations are numerically simulated using the Nactsheim-Swigert shooting technique together with Runge-Kutta six order iteration schemes. The velocity and temperature profiles are discussed and presented graphically. The comparison for dimensionless skin friction coefficient and local Nusselt number with previously published literature also take into account for the accuracy of the present analysis.

Keywords: MHD; mixed convection; nanofluid; heat generation; stagnation-point flow.

[*]Corresponding author: Email: mdshakhaoath.khan@uon.edu.au;

1. INTRODUCTION

Magneto-fluid-dynamics or hydro-magnetics is a limitless field of research which analyzed the study of the dynamics of electrically conducting fluids includes plasmas, liquid metals, and salt water or electrolytes etc. The expression magneto-hydrodynamics (MHD) is consists of three belongings such as magneto (magnetic field), hydro (liquid) and dynamics (movement of particles). As a consequence magnetic fields induce current flows in a dynamic fluid and create forces on the fluid and also adjust the magnetic field itself. The combination of the Navier-Stokes equations of fluid-mechanics and Maxwell's equations of electromagnetism consequently established MHD relations. Due to wide applications in heat exchangers, post accidental heat removal in nuclear reactors, geothermal and oil recovery, solar collectors, drying processes, building construction, etc. the Buoyancy flow [1] and heat transfer is a significant phenomenon in engineering systems.

To incorporate the importance regarding MHD there is some suitable references from the literature [2-5], that reports MHD Flow of Oldroyd-B Fluid, Maxwell Fluid, Jeffrey Fluid also carried out MHD slip flow analysis of non-Newtonian fluid over a shrinking surface.

Also as conventional heat transfer fluids, including oil, water, and ethylene glycol mixture are poor heat transfer fluids, since the thermal conductivity of these fluids plays important role on the heat transfer co-efficient between the heat transfer medium and the heat transfer surface.

The effects of heat generation arise in high temperature ingredients processing operations also it can affect on heat transfer over an extending surface [6]. Choi [7] was the first who employ a technique to improve heat transfer is by using nano-scale particles in the base fluid and introduced the term of nanofluids as a novel class of fluid. As a result this type of fluids determines high thermal conductivity, significant change in properties such as viscosity and specific heat in comparison to the base fluid. Shehzad et al. [8-10] investigated on the boundary layer flow of thermal conductivity and heat generation/absorption, power law heat flux, heat source an thermal radiation. The heat transfer and fluid flow due to buoyancy forces in a partially heated enclosure using different types of nanoparticles is carried out by Oztop and Abu-Nada [11]. They have also provided the thermo physical properties of the fluid and nanoparticles as shown in Table. 1. Goodarzi et al. [12] also carried out the mixed convective laminar and turbulent nanofluid in a shallow rectangular enclosure by using a two-phase mixture model.

Table 1. Thermophysical possessions of the fluid and the nanoparticles [11,12]

Physical properties	Fluid phase (water)	Cu	Al_2O_3	TiO_2
C_p(J/kgK)	4179	385	765	686.2
ρ(kg /m^3)	997.1	8933	3970	4250
k(W/mK)	0.613	400	40	8.9538
$\alpha \times 10^{-7}$ (m^2/ s)	1.47	1163.1	131.7	30.7
$\beta \times 10^{-7}$ (m^2/ s)	21	1.67	0.85	0.9

Nanofluid-technology is now largely used in engineering and industrial applications. Due to this applications in recent years many researchers investigates some numerical and experimental analysis on nanofluids include convective instability [13] thermal conductivity [14,15] and natural convective boundary-layer flow [16,17]. Recently boundary layer heat-mass transfer free convection flows also in porous media of a nanofluid past a stretched

sheet reported by Khan and Pop [18]. Hamad and Pop [19] studied MHD free convection rotating flow of a nanofluid. The boundary layer nanofluid flow with MHD radiative possessions recently predicted Md. Shakhaoath Khan et al. [20] analyzed. Khan and Pop [21] analyzed boundary layer heat and mass transfer analysis past a wedge moving in a nanofluid. Very recently Tamim et al. [22] investigates the mixed convection boundary layer flow of a nanofluid near the stagnation-point on a vertical plate where the mixed convection flows are characterized by the buoyancy parameter λ, whereas for assisting flow, λ > 0 and for opposing flow λ < 0. Thesame problem corresponds to forced convection flow when the buoyancy effects are negligible (λ = 0).

Recently there have been relatively few studies [23-32] that reports MHD boundary layer fluid as well as nanofluid flow as well.

The present study predicting the MHD mixed convection boundary layer flow of a nanofluid near the stagnation-point on a vertical plate with heat generation for both assisting and opposing flows. And this work extended the study of Tamimet et al. [22]. The governing equations are transformed into nonlinear ordinary differential equations which depend on the Magnetic parameter(M), buoyancy parameter(λ), Prandtl number(P_r), heat generation parameter (Q) and volume fraction parameter (φ).The obtained nonlinear coupled ordinary differential equations are solved numerically using Nactsheim-Swigert [33] shooting iteration technique together with Runge-Kutta six order iteration schemes. The velocity and temperature distributions are discussed and presented graphically. The comparison for dimensionless skin friction coefficient and local Nusselt number with Tamim et al. [22] also take into account for the accuracy of the present analysis.

2. FORMULATION OF THE PROBLEM

The steady two dimensional boundary layer mixed convection flow considered near the stagnation-point on a vertical flat plate. The physical configuration of this problem is shown in Fig. 1 [22]. No slip conditions occurs between the thermally equilibrium nanoparticles. Here the coordinate's *x*-axis is extending along the surface whereas the *y*-axis is measured normal to the surface.

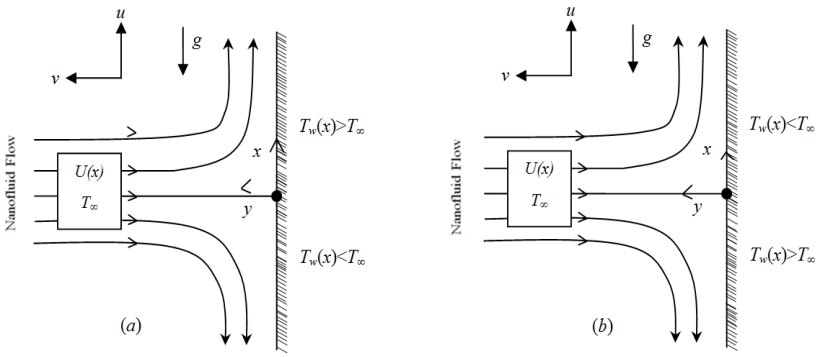

Fig. 1. Physical configuration and coordinates system

The outer boundary layer of the x-component velocity taken as $U(x) = ax$ where a is positive constants and the plate temperature taken as proportional to the distance from the

stagnation-point, $T_w(x)=T_\infty+bx$, whereas b>*0* indicates assisting flow which occurs when the superior pert of the plate is heated while the lower half of the plated is cooled. And *b<0* indicates opposing flow which occurs if the superior pert of the plate is cooled while the lower part of the plate is heated. Thus the buoyancy force arises here to assist the main flow field.

The governing equations for the laminar two-dimensional boundary layer heat transfer flow can be written as follows;

$$\frac{\partial u}{\partial x}+\frac{\partial v}{\partial y}=0, \tag{1}$$

$$u\frac{\partial u}{\partial x}+v\frac{\partial u}{\partial y}=U\frac{dU}{dx}+\frac{\mu_{nf}}{\rho_{nf}}\left(\frac{\partial^2 u}{\partial y^2}\right)+\frac{\left[\varphi\rho_S\beta_S+(1-\varphi)\rho_f\beta_f\right]g(T-T_\infty)}{\rho_{nf}}+\frac{\sigma B_0^{\,2}}{\rho}(U-u), \tag{2}$$

$$u\frac{\partial T}{\partial x}+v\frac{\partial T}{\partial y}=\alpha_{nf}\frac{\partial^2 T}{\partial y^2}+\frac{Q_\circ}{\rho_f C_p}(T-T_\infty), \tag{3}$$

Here, $\mu_{nf}$is the viscosity of the nanofluid, α_{nf} is the thermal diffusivity of the nanofluid and ρ_{nf} is the density of the nanofluid, β_f and β_s are the thermal expansion coefficients of the base fluid and nanoparticle, respectively. The values of μ_{nf},$\alpha_{nf}$and ρ_{nf}can be written as;

$$\begin{aligned}&\mu_{nf}=\frac{\mu_f}{(1-\varphi)^{2.5}},\ \rho_{nf}=(1-\varphi)\rho_f+\varphi\rho_s,\ \left(\rho C_p\right)_{nf}=(1-\varphi)\left(\rho C_p\right)_f+\varphi\left(\rho C_p\right)_s,\\&\alpha_{nf}=\frac{k_{nf}}{\left(\rho C_p\right)_{nf}},\frac{k_{nf}}{k_f}=\frac{\left(k_s+2k_f\right)-2\varphi\left(k_f-k_s\right)}{\left(k_s+2k_f\right)+\varphi\left(k_f-k_s\right)},\end{aligned} \tag{4}$$

Where, ρ_f and ρ_s is density of the base fluid and nanoparticle respectively, μ_f is viscosity of the base fluid, $k_f$and k_s is the thermal conductivity of the base fluid and nanoparticle respectively and k_{nf} is the effective thermal conductivity of the nanofluid approximated by the Maxwell-Garnett model [11].

The boundary condition for the model is;

$$\begin{aligned}&u=0,\ v=0,\ T=T_w(x)=T_\infty+bx \text{ at } y=0,\\&\quad u=U(x)=ax,\ T\to T_\infty \text{ as } y\to\infty.\end{aligned} \tag{5}$$

3. SOLUTION OF THE FLOW FIELD

In order to conquers a similarity solution to eqs. (1) to (3) with the boundary conditions (5) the following dimensionless variables are used;

$$\eta=y\sqrt{\frac{a}{\nu_f}},\ \psi=x\sqrt{a\nu_f}\,f(\eta),\ \theta=\theta(\eta)=\frac{T-T_\infty}{T_w-T_\infty} \text{ and } u=\frac{\partial\psi}{\partial y},\ v=-\frac{\partial\psi}{\partial x}. \tag{6}$$

From the above transformations the non-dimensional, nonlinear, coupled ordinary differential equations are obtained as;

$$f''' + (1-\varphi)^{2.5}\left(1-\varphi+\varphi\rho_S/\rho_P\right)\left[ff'' - f'^2 + 1 + \lambda\theta + M\left(1-f'\right)\right] = 0, \tag{7}$$

$$\theta'' + \left(P_r \frac{(1-\varphi)+\varphi\left(\rho C_p\right)_S/\left(\rho C_p\right)_f}{k_{nf}/k_f}\right)\left(f\theta' - f'\theta + Q\theta\right) = 0. \tag{8}$$

The transformed boundary conditions are as follows:

$$\left.\begin{array}{ll} f=0, f'=0, \theta=1 & at\ \eta=0 \\ f'=1, \theta=0 & as\ \eta\to\infty. \end{array}\right\} \tag{9}$$

Where the notation primes denote differentiation with respect to η and the parameters are defined as;

$M = \dfrac{\sigma B_0^{\,2}}{\rho a}$, Magnetic paramete

$\lambda = \dfrac{G_r}{\mathrm{Re}_x^{\,2}} = \dfrac{b\left[\varphi\rho_S\beta_S + (1-\varphi)\rho_f\beta_f\right]g}{\rho_{nf}a^2}$, Buoyancy/thermal convection parameter

$G_r = \dfrac{x^3\left[\varphi\rho_S\beta_S + (1-\varphi)\rho_f\beta_f\right]g(T_w - T_\infty)}{\rho_{nf}\nu_{nf}^2}$, localGrash of number

$\mathrm{Re}_x = \dfrac{xU(x)}{\nu_{nf}}$, local Reynolds number

$P_r = \dfrac{\upsilon_f}{\alpha_f}$ Prandtl number and

$Q = \dfrac{Q_\circ}{a\rho C_p}$, heat source parameter

The physical quantities of interest are the skin friction coefficient and the local Nusselt number can be obtained [22] as follows;

$$\begin{aligned} C_f\left[\mathrm{Re}_x\right]^{1/2} &= 2\frac{f''(0)}{(1-\varphi)^{2.5}}, \\ Nu_x\left[\mathrm{Re}_x\right]^{-1/2} &= -\frac{k_{nf}\theta'(0)}{k_f}. \end{aligned} \tag{10}$$

4. NUMERICAL SIMULATION

The non-dimensional, nonlinear, coupled ordinary differential eqs. (7) and (8) with boundary conditions (9) are solved numerically using the Nactsheim and Swigert [33] shooting iteration technique together with a sixth-order Runge-Kutta iteration scheme to determine the continuity, momentum and energy as a function of the independent variable, η. In this approach, the missing (unspecified) initial condition at the initial point of the interval is assumed and the differential equation is integrated numerically as an initial value problem to the terminal point. The accuracy of the assumed missing initial condition is then verified via comparison with the computed value of the dependent variable at the terminal point with its given value there. If a difference exists, another value of the missing initial condition must be assumed and the process is repeated. This process is continued until the agreement between the calculated and the given condition at the terminal point is within the specified degree of accuracy. Extension of the iteration shell to considered system of differential eqns. is straightforward; there are two asymptotic boundary condition and hence two unknown surface conditions $f'(0)$ and $\theta(0)$.

5. RESULTS AND DISCUSSION

The numerical values of velocity and temperature have been computed for the magnetic parameter, *M*, Thermal convective parameter, λ, Prandtl number, P_r heat generation parameter, *Q*, and volume fraction parameter, φ respectively. Among the parameters λ>0 for assisting flows, λ<0 for opposing flows and λ = 0 corresponding to forced convection when the buoyancy force is absent. Different nanofluid-particles as copper (Cu), alumina (Al_2O_3) and titania (TiO_2) are taken into account. To assess the accuracy of the numerical results the Skin friction coefficient and surface heat rate compared with previous literature [22] and shown in Table 2-4. And excellent agreement is observed from this comparison. Also a consequence has been found that the skin friction coefficient and local Nusselt number increase with increasing *λ & φ*.

Table 2. Comparison of the skin friction coefficient and the Nusselt number when *λ = 1, M*=0, and *Q=0*

Nanoparticle	φ	λ=1 (Assisting flow)			
		Tamim et al. [22]	Present Results	Tamim et al. [22]	Present Results
		$[Re_x]^{1/2}C_f$	$[Re_x]^{1/2}C_f$	$[Re_x]^{1/2}Nu_x$	$[Re_x]^{1/2}Nu_x$
Cu	0.00	3.05355	3.05687	1.65242	1.66482
	0.05	3.91833	3.91987	1.87279	1.89754
	0.10	4.81536	4.81754	2.08336	2.08458
	0.15	5.77580	5.79630	2.29008	2.29145
	0.20	6.82739	6.84644	2.49642	2.49783
Al_2O_3	0.00	3.05355	3.05683	1.65242	1.66092
	0.05	3.51805	3.52584	1.80652	1.81547
	0.10	4.02763	4.02359	1.96055	1.97580
	0.15	4.59295	4.59578	2.11528	2.12254
	0.20	5.22693	5.22699	2.27145	2.28654
TiO_2	0.00	3.05355	3.05482	1.65242	1.66874
	0.05	3.53844	3.53963	1.78590	1.79872
	0.10	4.06820	4.06899	1.91667	1.92547
	0.15	4.65406	4.65546	2.04529	2.04689
	0.20	5.30940	5.31205	2.17213	2.17321

Table 3. Comparison of the skin friction coefficient and the Nusselt number when λ = 0, *M*=0, and *Q=0*

Nanoparticle	φ	λ = 0 (Forced convection)			
		Tamim et al. [22]	Present Results	Tamim et al. [22]	Present Results
		$[Re_x]^{1/2}C_f$	$[Re_x]^{1/2}C_f$	$[Re_x]^{1/2}Nu_x$	$[Re_x]^{1/2}Nu_x$
Cu	0.00	2.46518	2.47584	1.57343	1.58741
	0.05	3.10770	3.11459	1.77577	1.78421
	0.10	3.76865	3.78452	1.96921	1.97710
	0.15	4.47381	4.49874	2.15931	2.16879
	0.20	5.24549	5.25568	2.34936	2.35510
Al_2O_3	0.00	2.46518	2.47412	1.57343	1.58741
	0.05	2.81753	2.82568	1.71690	1.72201
	0.10	3.20411	3.21254	1.86033	1.87405
	0.15	3.63365	3.64582	2.00450	2.01373
	0.20	4.11665	4.12658	2.15020	2.16687
TiO_2	0.00	2.46518	2.47178	1.57343	1.58957
	0.05	2.83469	2.84581	1.69742	1.69987
	0.10	3.23858	3.24410	1.81898	1.82574
	0.15	3.68615	3.69870	1.93870	1.94783
	0.20	4.18844	4.19973	2.05698	2.06547

Fig. 2 depicts the velocity profiles for different values of naoparticles and magnetic parameter, *M* when λ = 2 (assisting flow). As a result, the momentum boundary layer thickness increases. It is evident from these figures that velocity profiles satisfy the far field boundary conditions asymptotically and validated the numerical results.

Table 4. Comparison of the skin friction coefficient and the nusselt number when λ = -1, *M*=0, and *Q=0*

Nanoparticle	φ	λ =-1 (Opposing flow)			
		Tamim et al [22]	Present Results	Tamim et al. [22]	Present Results
		$[Re_x]^{1/2}C_f$	$[Re_x]^{1/2}C_f$	$[Re_x]^{1/2}Nu_x$	$[Re_x]^{1/2}Nu_x$
Cu	0.00	1.82621	1.83584	1.47787	1.48741
	0.05	2.22075	2.23257	1.65618	1.66254
	0.10	2.61683	2.62250	1.82647	1.83102
	0.15	3.03459	3.05471	1.99394	1.99871
	0.20	3.49056	3.49910	2.16169	2.18457
Al_2O_3	0.00	1.82621	1.83258	1.47787	1.49542
	0.05	2.05421	2.07582	1.60756	1.61287
	0.10	2.30424	2.30871	1.73719	1.74410
	0.15	2.58292	2.59651	1.86760	1.87412
	0.20	2.89819	2.89993	1.99963	2.00478
TiO_2	0.00	1.82621	1.83247	1.47787	1.48974
	0.05	2.06795	2.07412	1.58950	1.59952
	0.10	2.33229	2.34127	1.69904	1.71243
	0.15	2.62650	2.63658	1.80712	1.81470
	0.20	2.95913	2.96524	1.91423	1.92105

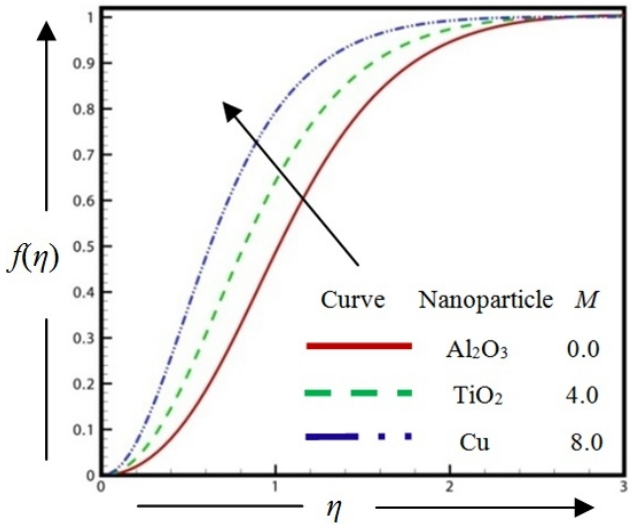

Fig. 2. Velocity distribution for different types of nanoparticle and M where φ=0.3, λ =2.0, P_r=0.71& Q=1.0

Fig. 3 represents the temperature profiles for different values of naoparticles and prandtl number P_r, when λ = 2 (assisting flow). It was found the temperature boundary layer decreases as Prandtl number increases.

The effect of the heat generation and different nanoparicle on velocity and temperature distributions in the case of λ = 0 (forced convection) are illustrated in Figs. 4 and 5, respectively. It is observed that the momentum boundary layer thickness increases while the thermal boundary layer decreases as the heat generation growths.

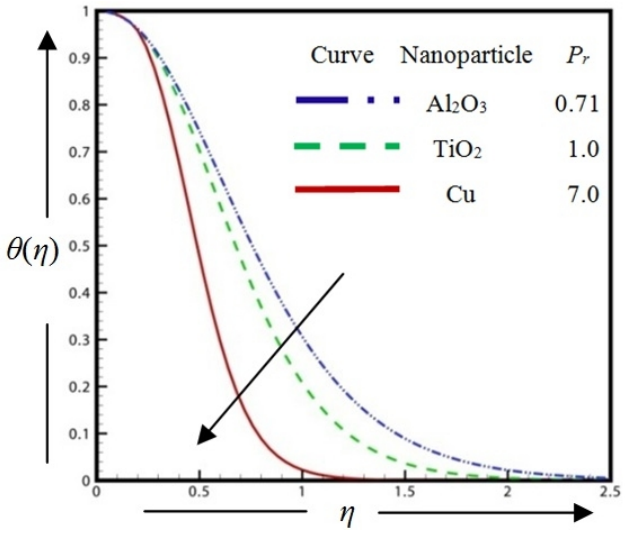

Fig. 3. Temperature distribution for different types of nanoparticle and P_r where φ=0.3, λ =2.0, Q=1.0& M=4.0

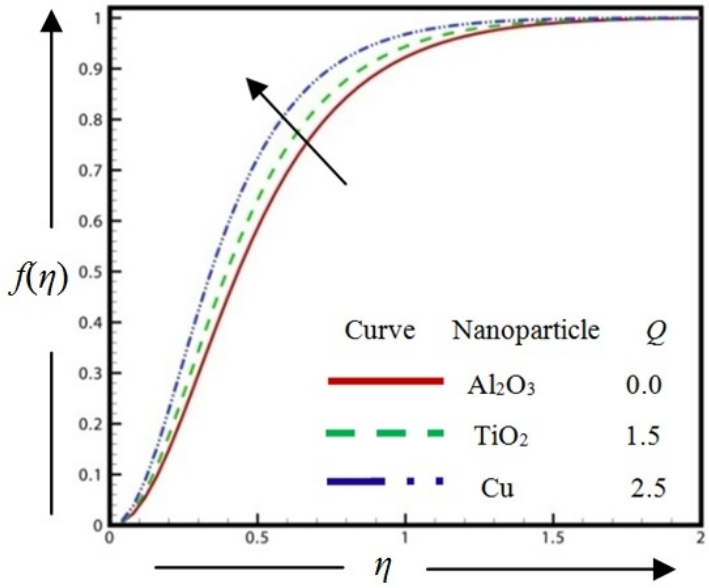

Fig. 4. Velocity distribution for different types of nanoparticle and *Q* where φ=*0.3, λ =0.0, P_r=0.71 &M=4.0*

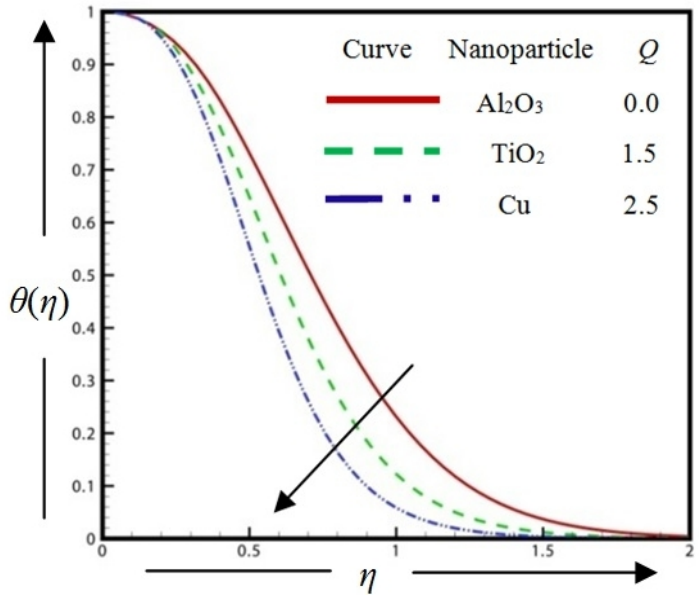

Fig. 5. Temperature distribution for different types of nanoparticle and *Q* where φ=*0.3, λ =0.0, P_r=0.71 & M=4.0*

Fig. 6 show the velocity profiles for various values of the volume fraction parameter φ in the case of titania (TiO_2)-water when λ = -2 (opposing flow). It is noted that due to the fact that the presence of nano-solid-particles leads to further diminishing of the boundary layer the momentum boundary layer thickness increases with the volume fraction parameter.

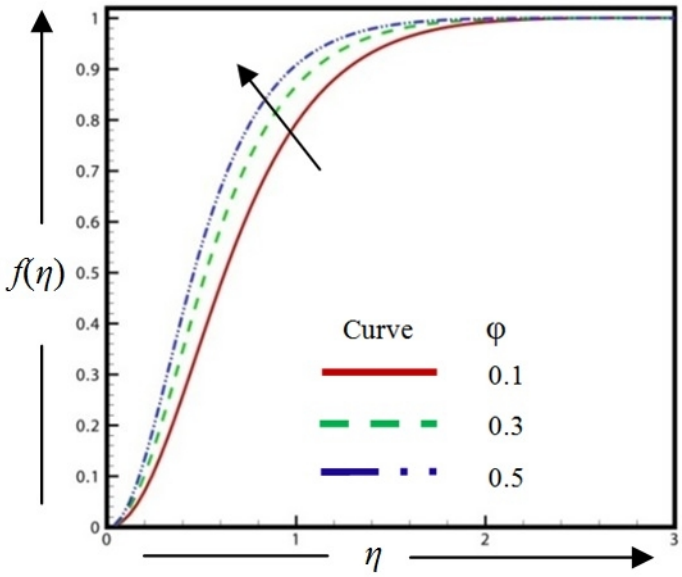

Fig. 6. Velocity distribution for different types of volume fraction parameter, φ where Q=1.0, λ =-2.0, P_r=0.71 & M=4.0

Fig. 7 is presented to show the effect of the TiO_2 nanoparticle volume fraction on temperature distribution. From this figure, when the volume of TiO_2 nanoparticles increases, the thermal conductivity increases, and then the thermal boundary layer thickness increases progressively.

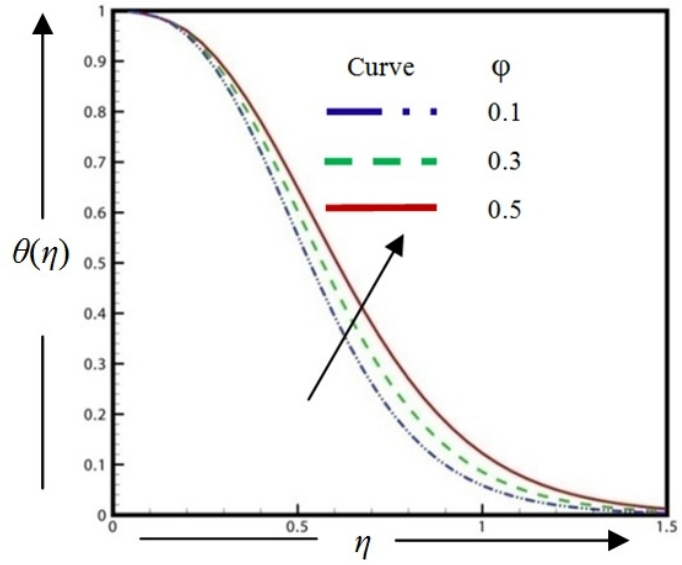

Fig. 7. Temperature distribution for different types of volume fraction parameter, φ where Q=1.0, λ =-2.0, P_r=0.71 & M=4.0

6. CONCLUDING REMARKS

Magnetohydroynamics mixed convection boundary layer heat transfer flow of a nanofluid near the stagnation-point on a vertical plate with the effect of heat generation has been studied. Heat transfer characteristics of copper (Cu), alumina (Al_2O_3) and titania (TiO_2) nanoparticles is observed. The momentum boundary layer thickness increases for all cases. The temperature boundary layer thickness is going down for varying different types of nanoparticle, increasing heat generation and Prandtl number respectively. But at higher volume fraction parameter the temperature boundary layer thickness rises gradually. The current study has applications in high-temperature nano-technological materials processing.

7. NOMENCLATURE

a, b constant
Al_2O_3 alumina
B_0 magnetic induction
C_f Skin friction coefficient
C_P specific heat at constant pressure
Cu copper
G_r Grashof number
k thermal conductivity
M magnetic parameter
Nu_x Local Nusselt number
P fluid pressure
P_r Prandtl number
Q heat source parameter
Q_0 heat generation constant
Re_x Local Reynolds number
T temperature at the surface
T_∞ ambient temperature as $y \to \infty$
TiO_2 titania
u,v velocity components along x, y axes respectively
$U(x)$ free stream velocity

8. Greek Symbols

ν kinematic viscosity
ρ density
σ conductivity of the material
α thermal diffusivity
β co-efficient of thermal expansion
λ Buoyancy/thermal convection parameter
μ dynamic viscosity
η similarity variable
τ_w Wall shear stress
ψ stream function
φ volume fraction parameter
$f'(\eta)$ dimensionless velocity
$\theta(\eta)$ dimensionless temperature

ACKNOWLEDGEMENTS

The authors are very thankful to the editor and reviewers for their constructive comments and valuable suggestions to improve this research paper.

COMPETING INTERESTS

Authors have declared that no competing interests exist.

REFERENCES

1. Ostrach S. Natural convection in enclosures. J. Heat Transfer. 1988;110:1175–1190.
2. Hayat T, Shehzady SA, Mustafaz M, Hendi A. MHD Flow of an Oldroyd-B Fluid through a Porous Channel. International Journal of Chemical Reactor Engineering. 2012;10:A8.
3. Shehzad SA, Ahmad A, Hayat T. Hydromagnetic Steady Flow of Maxwell Fluid over a Bidirectional Stretching Surface with Prescribed Surface Temperature and Prescribed Surface Heat Flux. Plos One. 2013;8:68139.
4. Shehzad SA, Alsaedi A, Hayat T. Influence of Thermophoresis and Joule Heating on The Radiative Flow of Jeffrey Fluid With Mixed Convection. Brazilian Journal of Chemical Engineering. 2013;30:897-908.
5. Turkyilmazoglu M. Dual and triple solutions for MHD slip flow of non-Newtonian fluid over a shrinking surface. Comput. Fluids. 2012;70:53-58.
6. Vajravelu K, Hadjinicalaou A. Heat transfer in a viscous fluid over a stretching sheet with viscous dissipation and internal heat generation. Int. Comm. Heat Mass Trans. 1993;20:417-430.
7. Choi SUS. Enhancing Thermal Conductivity of Fluids with Nanoparticles, Development and Applications of Non- Newtonian Flows. Siginer DA, Wang HP. eds., ASME MD-, USDOE, Washington, DC (United States). 1995;(231)66:99-105.
8. Shehzad SA, Alsaedi A, Hayat T, Alhuthali MS. Three-Dimensional Flow of an Oldroyd-B Fluid with Variable Thermal Conductivity and Heat Generation/Absorption. Plos One. 2013;8:78240.
9. Shehzad SA, Qasim M, Hayat T, Sajid M, Obaidat S. Boundary layer flow of Maxwell fluid with power law heat flux and heat source. International Journal of Numerical Methods for Heat & Fluid Flow. 2013;23(7):1225–1241.
10. Shehzad SA. MHD mixed convection flow of thixotropic fluid with thermal radiation. Heat Transfer Research. 2013;44:687-702.
11. Oztop HF, Abu-Nada E. Numerical study of natural convection in partially heated rectangular enclosures filled with nanofluids. International Journal of Heat and Fluid Flow. 2008;29:1326–1336.
12. Goodarzi M, Safaei MR, Ahmadi G, Vafai K, Dahari M, Jomhari N, Kazi SN. An Investigation of Laminar and Turbulent Nanofluid Mixed Convection in a Shallow Rectangular EnclosureUsing a Two-phase Mixture Model. International Journal of Thermal Sciences. 2014;75:204-220.
13. Kang Ki JYT, Choi CK. Analysis of convective instability and heat transfer characteristics of nanofluids. Phys. Fluids. 2004;16:2395-2401.
14. Kang HU, Kim SH, Oh JM. Estimation of thermal conductivity of nanofluid using experimental effective particle volume. Exp. Heat Transfer. 2006;19:181-191.
15. Jang SP, Choi SUS. Effects of various parameters on nanofluid thermal conductivity. ASME J. Heat Transfer. 2007;129: 617-623.

16. Nield A, Kuznetsov AV. The Cheng–Minkowycz problem for natural convective boundary-layer flow in a porous medium saturated by a nanofluid. Int. J. Heat and Mass Transfer. 2009;52:792–5795.
17. Kuznetsov AV, Nield DA. Natural convective boundary-layer flow of a nanofluid past a vertical plate. Int. J. of Thermal Sci. 2010;49:243 -247.
18. Khan WA, Pop I. Free convection boundary layer flow past a horizontal flat plate embedded in a porous medium filled with a nanofluid. ASME J. Heat Transfer. 2011;133:157-163.
19. Hamad MAA, Pop I. Unsteady MHD free convection flow past a vertical permeable flat plate in a rotating frame of reference with constant heat surface in a nanofluid. Heat Mass Transfer. 2012;47:1517-1524.
20. Khan MS, Alam MM, Ferdows M. Effects of Magnetic field on Radiative flow of a Nanofluid past a Stretching Sheet. Procedia Engineering Elsevier. 2013;56:316-322.
21. Khan WA, Pop I. Boundary Layer Flow Past a Wedge Moving in a Nanofluid. Mathematical Problems in Engineering. 2013;1-7.
22. Tamim H, Dinarvand PPS, Hosseini PPR, Khalili PS, Khalili PA. Mixed Convection Boundary-layer Flow of a Nanofluid Near Stagnation-point on a Vertical Plate with Effects of Buoyancy Assisting and Opposing Flows. Research Journal of Applied Sciences, Engineering and Technology. 2013;6:1785-1793.
23. Khan MS, Alam MM, Ferdows M. Finite Difference Solution of MHD Radiative Boundary Layer Flow of a Nanofluid past a Stretching Sheet. Proceeding of the International Conference of Mechanical Engineering. FL-011, BUET, Dhaka, Bangladesh; 2011.
24. Khan MS, Alam MM, Ferdows M. MHD Radiative Boundary Layer Flow of a Nanofluid past a Stretching Sheet. Proceeding of the International Conference of Mechanical Engineering and Renewable Energy. PI-105, CUET,Chittagong, Bangladesh; 2011.
25. Khan MS, Karim Ifsana, Ali LE, Islam A. MHD Free Convection Boundary layer Unsteady Flow of a Nanofluid along a stretching sheet with thermal Radiation and Viscous Dissipation Effects. International Nano Letters. 2012;2:24.
26. Ferdows M, Khan, MS, Alam MM, Sun S. MHD Mixed convective boundary layer flow of a nanofluid through a porous medium due to an Exponentially Stretching sheet. Mathematical problems in Engineering. 2012;3:2551-1557.
27. Khan MS, Wahiduzzaman M, Sazad MAK, Uddin MS. Finite difference solution of MHD free convection heat and mass transfer flow of a nanofluid along a Stretching sheet with Heat generation effects. Indian Journal of Theoretical Physics. 2012;60:285-306.
28. Ferdows M, Khan MS, Alam MM, Bég OA. Numerical Study of Transient Magnetohydrodynamic Radiative Free Convection Nanofluid Flow from a Stretching Permeable Surface. Journal of Process Mechanical Engineering. 2013;1-16.
29. Beg OA, Khan MS, Karim Ifsana, Ferdows M, Alam MM. Explicit Numerical study of Unsteady Hydromagnetic Mixed Convective Nanofluid flow from an Exponential Stretching sheet in Porous media. Applied Nanoscience; 2013.
30. Khan MS, Karim Ifsana, Biswas MHA. Heat Generation, Thermal Radiation and Chemical Reaction Effects on MHD Mixed Convection Flow over an Unsteady Stretching Permeable Surface. International Journal of Basic and Applied Science. 2012;1(2):363-377.
31. Khan MS, Karim Ifsana, Biswas MHA. Non-Newtonian MHD Mixed Convective Power-Law Fluid Flow over a Vertical Stretching Sheet with Thermal Radiation, Heat Generation and Chemical Reaction Effects. Academic Research International. 2012;3(3):80-92.

32. Khan MS, Karim Ifsana, Islam MS. Possessions of Chemical Reaction on MHD Heat and Mass Transfer Nanofluid Flow on a Continuously Moving Surface. American Chemical Science Journal. 2014;4(3):401-415.
33. Nachtsheim PR, Swigert P. Satisfaction of the asymptotic boundary conditions in numerical solution of the system of non-linear equations of boundary layer type. *NASA*, TND-3004; 1965.

Peer-review history:
The peer review history for this paper can be accessed here:
http://www.sciencedomain.org/review-history.php?iid=476&id=33&aid=4113